Cellular Immunology 337 (2019) 22–32

Contents lists available at ScienceDirect

Cellular Immunology

journal homepage: www.elsevier.com/locate/ycimm

Research paper

# MiR-129-3p favors intracellular BCG survival in RAW264.7 cells by inhibiting autophagy via Atg4b

Yuliang Qu[a,b], Shuqin Ding[c], Zhanbing Ma[d], Dan Jiang[a,b], Xiangrong Xu[d], Ying Zhang[e], Aijun Zhang[b,d,*], Guangxian Xu[b,d,*]

[a] Department of Clinical Medicine, School of Clinical Medicine, Ningxia Medical University, Yinchuan 750004, China
[b] Ningxia Key Laboratory of Clinical and Pathogenic Microbiology, General Hospital of Ningxia Medical University, Yinchuan 750004, China
[c] Department of Medical Laboratory, School of Clinical Medicine, Ningxia Medical University, Yinchuan 750004, China
[d] Department of Medical Genetic and Cell Biology, College of Basic Medicine, Ningxia Medical University, Yinchuan 750004, China
[e] Department of Molecular Microbiology and Immunology, Bloomberg School of Public Health, Johns Hopkins University, Baltimore, MD 21205, USA

ARTICLE INFO

*Keywords:*
MiR-129-3p
Atg4b
Autophagy
MTB

ABSTRACT

Autophagy plays an important role in the fight against *Mycobacterium tuberculosis* infection. Massive researches proved that miRNAs could be the regulators of autophagy, which implied miRNAs could favor MTB invasion or latent infection. In our study, multiple bioinformatics databases and software were used to seek and lock the miRNAs associating with regulation of autophagy. Notably, a novel miR-129-3p was found and its target gene Atg4b showed grand potential in mediation of autophagy. Moreover, BCG infection triggered miR-129-3p overexpression in RAW264.7 cells. Up-regulation of miR-129-3p decreased mRNA or protein level of Atg4b and resulted in the inhibition of autophagy. The antagomir of miR-129-3p had the opposite impact. The LC3 puncta formation in RAW264.7 cells were also affected after transfection of miR-129-3p mimic or antagomir. The mRFP-GFP-LC3 analysis indicated that mimic of miR-129-3p impaired autophagic flux while antagomir improved autophagy. The CFU assay results showed that miR-129-3p promoted the intracellular survival of BCG in macrophages. Consequently, these data suggested that miR-129-3p could favor MTB survival by inhibiting autophagy via Atg4b.

## 1. Introduction

*Mycobacterium tuberculosis* (M. *tuberculosis*), the causative agent of tuberculosis, can survive within macrophages and leads to latent infection. Many researches indicate MTB can evade host antimicrobial responses of immune system [1,2]. In this process, the emerging roles of miRNAs are sort of two-blade swords. Sometimes, miRNAs are defenders against MTB by facilitating autophagy through targeting different genes [3,4]. In some cases, miRNAs are accomplices of MTB infection by inhibiting host antimicrobial reacting [5]. Since the macrophages are the first defense line against MTB, the defensive mechanism especially the regulation of autophagy is the most concentrated in our study.

MiRNAs are under the spotlight for decades since the very beginning of their discovery. These small non-coding RNAs which are approximately 21 to 25 nucleotides in length, can control the expression of almost 30% of protein-coding genes by interacting with their mRNA, resulting in impair of translation [6]. In addition, the manner of miRNAs expression could be helpful as biomarkers for cancer or MTB infection [7]. Increasing reports suggest that miRNAs works in various aspects including cancer-related cell transformation, apoptosis or inflammation [8–10]. Recently, miR-155 was presented a new role as a key regulator of autophagy via dysregulation of MTOR pathway [11]. MiR-144 could inhibit antimicrobial responses by targeting autophagy protein DRAM2 [12]. Another study revealed that members of the miR-148/-152 family might represent prognostic markers and/or potential therapeutic targets for multiple types of cancer [13,14]. Thus, the precise role of miRNAs in different biological process is worthy to study.

Bioinformatics is a field contains diverse software tools and methods, which can narrow the range of massive biological data. In our research, multiple tools were used. For instance, functional pathways were analyzed by the Database for Annotation Visualization and Integrated Discovery (DAVID). DAVID is a tool of bioinformatics

* Corresponding authors at: Ningxia Key Laboratory of Clinical and Pathogenic Microbiology, General Hospital of Ningxia Medical University, Yinchuan 750004, China.
*E-mail addresses:* zhangaijun770316@sina.com (A. Zhang), xuguangxian@nxmu.edu.cn (G. Xu).

https://doi.org/10.1016/j.cellimm.2019.01.004
Received 6 October 2018; Received in revised form 19 January 2019; Accepted 25 January 2019
Available online 28 January 2019
0008-8749/ 

resources which aims to provide functional interpretation of large lists of genes derived from genomic studies [15]. Our previous research has found lots of miRNAs which were differentially expressed in rapamycin or 3-MA treated RAW264.7 cells comparing with control through RNA-sequencing technology [16]. In consideration of the upcoming widespread use of RNA-sequencing, our purpose is to provide a systematic way of bioinformatics analysis especially in screening miRNAs that correlated with autophagy are required illustration intensively.

Macroautophagy (referred to as autophagy) is a vital mechanism responsible for intracellular cycling of nutrient and resistance to pathogenic infection, which was found a half century ago. The autophagic process contains two major steps: formation of autophagosomes, maturation of autolysosome [17]. Since autophagy plays important roles in the axis of maintaining intracellular conditions, it can be regulated by dynamic pathways or cytokines [18,19]. Massive proofs show that the mammalian target of rapamycin complex 1(mTOR1) can promote autophagy by inhibiting ULK1 [20]. Notably, autophagy can be impacted by Beclin1, which is a scaffold of Beclin1-associated PI3P-kinase class III (PI3KC3) recruiting active or inhibiting factors like UVRAG [21,22]. Importantly, overexpression of IFNG can induce autophagy by triggering Jak-STAT pathway [23]. Meanwhile, there are over 30 distinct autophagy-related genes (ATGs) being reported so far. Among ATGs, Atg4 contributes to converting LC3I into LC3II by cutting off C-terminal last five amino acids of LC3 and regulates protein transport [24]. Atg16 with a mutation fails to localize to the pre-autophagosomal structure or interact with Atg5, suggest that their combination is crucial to the performance of roles in autophagy [25]. Autophagy was also regarded as a surveillance which can sense signals from various sources including hypoxia, fatty acid, starvation and components of bacterial surface especially on MTB [5,11,26]. The research indicates miRNAs circuit can be used by MTB to inhibit autophagy and reprogram host lipid metabolism to enable intracellular survival and persistence in the host [5].

In this study, we found a novel autophagy-related miR-129-3p through RNA sequencing as well as bioinformatics analysis. All genes function or pathway associating with autophagy was annotated via DAVID. Eventually, miR-129-3p was predicted and proved to mediate autophagic process by targeting Atg4b and favors MTB survival within macrophages.

## 2. Results

### 2.1. Differential expression of miRNAs through RNA sequencing

The RNA sequencing results showed that 20 miRNAs were significantly increased or decreased in RAW264.7 cells after treated with rapamycin or 3-MA. As shown in Fig. 1A, one of the miRNA clusters (from mmu-miR-152-5p to mmu-miR-215-5p) showed parallelly expressional trend. In addition, miR-182-3p, miR-20a and miR-129-5p in this cluster had already been proved to be regulators of autophagy through different ways [16,38,39]. Thus, we presumed that the rest miRNAs in the cluster (such as miR-129-3p) might be involved in regulation of autophagy. Notably, miR-129-3p expression was increased after treated with rapamycin indicating that it might play a role in rapamycin induced autophagy.

### 2.2. Bioinformatics analysis of miRNAs' target genes

14570 genes, the predicted target genes of 20 miRNAs, were obtained by using miRWalk 3.0. All genes were uploaded to DAVID software to identify GO categories and KEGG pathways. The partial results of GO term enrichment and KEGG analysis are provided in Table 1 (The top five of biological process contains transcription, DNA-templated (GO: 0006351), transport (GO: 0006810), regulation of transcription, DNA-templated (GO: 0006355), multicellular organism development (GO: 0007275), positive regulation of transcription from RNA polymerase II promoter (GO: 004944). First three of cellular component includes membrane (GO: 0016020), cytoplasm (GO: 0005737), nucleus (GO: 0005634)). The regulation of autophagy in MTB infection is a complex process caused by different genes. The autophagy-related GO enrichment which contained 21 terms covering 5560(1626 genes in biological process and 3934 genes in cellular component) genes arouse our interests (Fig. 2A). Meanwhile, KEGG analysis of 14570 genes revealed that there were 294 pathways enriched (Fig. 2B), and 18 (mmu05152: Tuberculosis, mmu04010: MAPK signaling pathway, mmu04152: AMPK signaling pathway, mmu04310: Wnt signaling pathway, mmu04630: Jak-STAT signaling pathway, mmu04068: FoxO signaling pathway, mmu04350: TGF-beta signaling pathway, mmu04150: mTOR signaling pathway, mmu04210: Apoptosis, mmu04620: Toll-like receptor signaling pathway, mmu04668: TNF signaling pathway, mmu04062: Chemokine signaling pathway, mmu04115: p53 signaling pathway, mmu04142: Lysosome, mmu04151: PI3K-Akt signaling pathway, mmu04145: Phagosome, mmu04064: NF-kappa B signaling pathway, mmu04140: Regulation of autophagy.) of 294 pathways were founded to be responsible for mediation of autophagy (Fig. 2B). Among these genes, miR-129-3p and its target gene Atg4b were further confirmed by using three conventional databases (miRanda, miRDB and TargetScan). As shown in Fig. 2C, the intersection of three different databases contained 91 genes, and the Atg4b was on the top-ten list of these genes (Fig. 2C) which also confirmed the results of miRWalk 3.0. The GO enrichment and KEGG analysis of Atg4b were provided in Table 2. The STRING database was recruited to verify the protein connection between Atg4b and other autophagic regulators, and Atg4b was strongly correlated with other genes (Fig. 2D). Taken together, miR-129-3p and Atg4b were predicted to play crucial roles in regulation of autophagy.

### 2.3. BCG infection triggers miR-129-3p expression in RAW264.7 cell

To confirm the bioinformatics analysis results, miR-129-3p expression in RAW264.7 cells was measured by qRT-PCR. The expression of miR-129-3p in rapamycin treated group was significantly increased (Fig. 3A) which was in accord with our RNA sequencing results. Many studies suggested that MTB infection could trigger abnormal expression of miRNAs [4,8,11]. To explore whether miR-129-3p is associated with MTB infection, we detected miR-129-3p expression in RAW264.7 cells after BCG infection at different MOI (1 or 10) and determined time. The expression of miR-129-3p was increased along with the amount of BCG (Fig. 3B). Moreover, the expression miR-129-3p reached highest level at 12 h after infection and began to fall after 24 h (Fig. 3C), indicating that miR-129-3p could be a symbol of MTB infection.

### 2.4. MiR-129-3p reduce Atg4b expression by interacting of its 3′UTR

Basing on bioinformatics analysis, the 3′UTR of Atg4b was matched with miR-129-3p seed region (Fig. 4A). Dual-luciferase report assays results indicated that overexpression of miR-129-3p impaired luciferase activity in 293 T cells containing Atg4b-WT vector but had little effect in those cells transfected with Atg4b-Mut vector (Fig. 4B). In contrast, this trend could be converted when antagomir replace the mimic of miR-129-3p, but still failed to affect luciferase activity in 293 T cells containing Atg4b-Mut vector (Fig. 4B). Before further studying in RAW264.7 cells, the transfection efficiency was tested. QRT-PCR data in Fig. 4C implied that the expression level of miR-129-3p was significantly increased in RAW264.7 cells after transfected with mimic of miR-129-3p and declined when antagomir transfected (Fig. 4C). Furthermore, qRT-PCR and western blotting assays were used to detect the impact of miR-129-3p on Atg4b expression both in mRNA and protein levels. As shown in Fig. 4D, the mRNA level was reduced after transfected with mimic of miR-129-3p, and vice versa (Fig. 4D). Meanwhile, the western blot detection showed that Atg4b expression was depressed after transfected with miR-129-3p mimic (Fig. 4E). Transfection of miR-129-3p antagomir promoted the expression of Atg4b in RAW264.7 cells

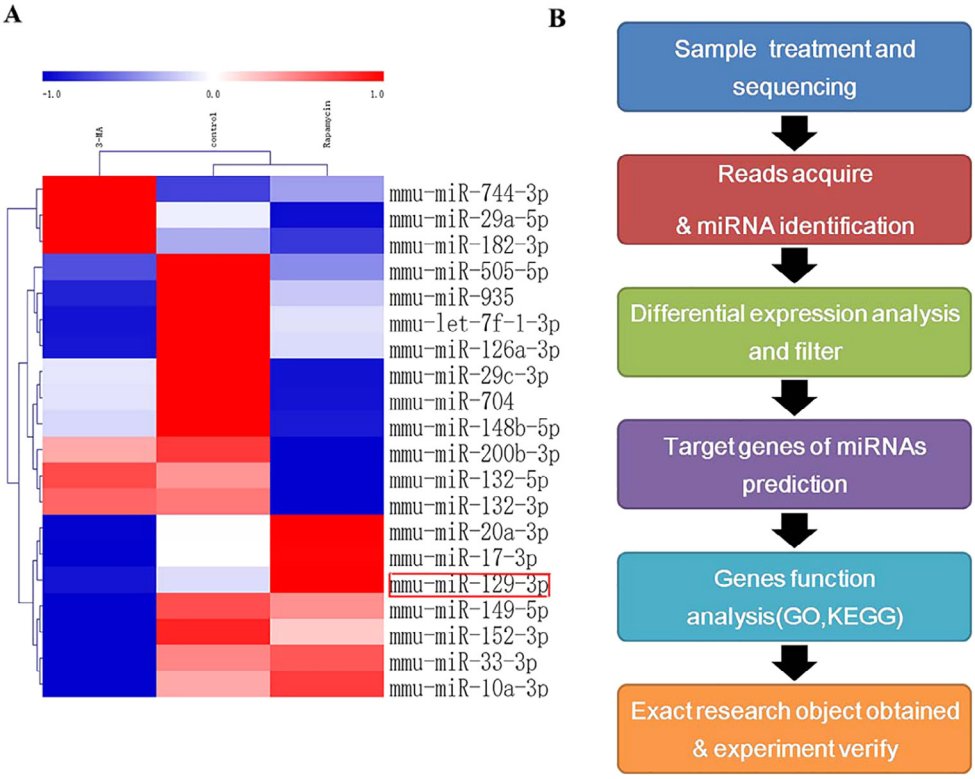


**Fig. 1.** Differential expression of miRNAs acquired by RNA sequencing. (A) Heatmap of the RNA-sequencing results including 20 miRNAs and their expression in different treatment (rapamycin or 3-MA). The red represents high expression and blue stand for low expression. (B) The procedure of bioinformatics analysis and main content of each step.

(Fig. 4G). The western blot results were also in accord with the intensity analyzed by Image J software (Fig. 4F, H). In conclusion, these results indicated that miR-129-3p suppressed expression of Atg4b by targeting its 3′UTR.

### 2.5. MiR-129-3p suppresses autophagy in RAW264.7 cells by inhibiting Atg4b

RAW264.7 cells transfected with control, miR-129-3p mimic or antagomir were furtherly infected with or without. Significantly, the mimic of miR-129-3p contributed decrease of Atg4b protein expression in uninfected and BCG-infected RAW264.7 cells while antagomir brought an increase in both treatments (Fig. 5A, B). Moreover, the accumulation of p62 protein was enhanced in mimic group (Fig. 5A, B). Meanwhile, miR-129-3p mimic decreased LC3II/I ratio while antagomir contributed to promotion of LC3II/I ratio in uninfected group (Fig. 5A). Interestingly, in BCG infected group, LC3-I level was decreased or increased more notably than changes of LC3-II levels (Fig. 5B), which indicating that Atg4b may play a role in the process of proLC3 converting to LC3-I. Furthermore, transfection with Atg4b siRNA significantly reduced the expression of Atg4b and both of LC3-I and LC3- II in RAW264.7 (Fig. 5C, D). What's more, miR-129-3p mimic could strengthen suppression of Atg4b expression caused by SiRNA. However, the antagomir of miR-129-3p could not elevate LC3-I/II expression (Fig. 5C, D) which also suggesting Atg4b was the target was miR-129-3p. For immunofluorescence analysis, RAW264.7 cells were transfected with miR-129-3p mimic or antagomir for 24 h, and then treated with rapamycin for 2 h. As shown in Fig. 6A, the puncta of LC3 were significantly decreased in miR-129-3p mimic group. Contrastly, the antagomir of miR-129-3p improved the quantity of LC3 puncta (Fig. 6A); the puncta counting confirmed these results (Fig. 6B). In conclusion, miR-129-3p impaired autophagy via Atg4b.

### 2.6. MiR-129-3p restrains phagosome formation and favors BCG survival

To figure out which stages that miR-129-3p impact on autophagy, the mRFP-GFP-LC3 cells were transfected with miR-129-3p mimic or antagomir for 24 h. The Immunofluorescence analysis indicated that the mimic of miR-129-3p decreased the red puncta, revealing miR-129-3p impaired the autophagic flux (Fig. 7A, B). Both red and yellow puncta were upregulated after transfection of miR-129-3p antagomir, suggesting that autophagic flux were increased and the phagosome formation was improved (Fig. 7A, B). The RAW264.7 cells were transfected with control, mimic or antagomir of miR-129-3p, and then treated with rapamycin or infected by MTB. The MTB survival within macrophages measured by CFU assay suggested that the mimic of miR-

**Table 1**
Partial results of GO term enrichment.

| Category | Term | Count | P-Value |
|---|---|---|---|
| GOTERM_BP | GO:0006351 ~ transcription, DNA-templated | 1075 | 1.22E−24 |
| GOTERM_BP | GO:0006810 ~ transport | 875 | 8.70E−21 |
| GOTERM_BP | GO:0006355 ~ regulation of transcription, DNA-templated | 793 | 2.21E−13 |
| GOTERM_BP | GO:0007275 ~ multicellular organism development | 728 | 2.17E−10 |
| GOTERM_BP | GO:0045944 ~ positive regulation of transcription from RNA polymerase II promoter | 513 | 1.61E−08 |
| GOTERM_CC | GO:0016020 ~ membrane | 3255 | 1.60E−47 |
| GOTERM_CC | GO:0005737 ~ cytoplasm | 3014 | 7.40E−41 |
| GOTERM_CC | GO:0005634 ~ nucleus | 2711 | 9.65E−25 |

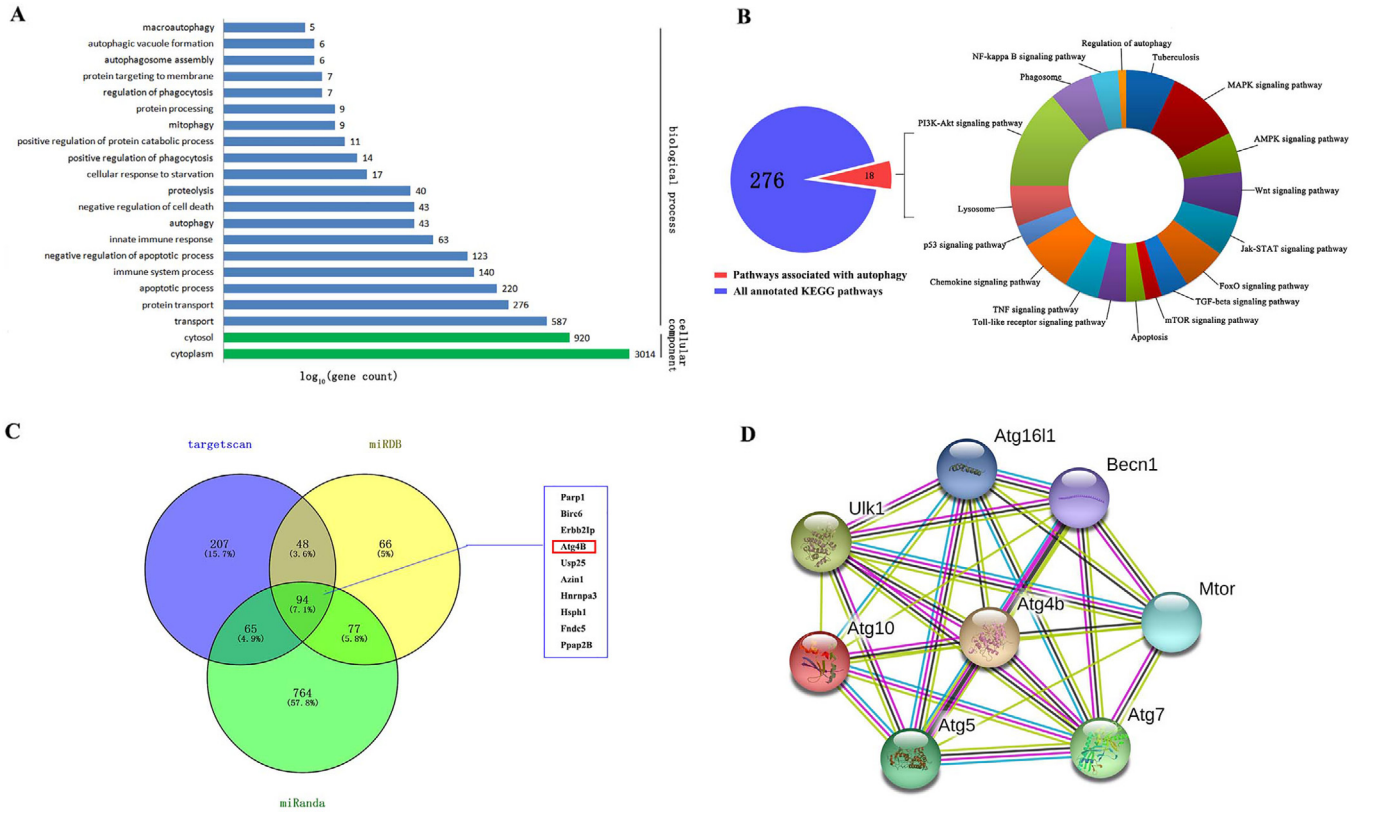


**Fig. 2.** Bioinformatics analysis of miRNAs' target genes. (A) Autophagy-related genes gained by GO enrichment, including 19 biological processes and 2 cellular components. (B) 294 pathways were annotated and including 18 pathways relating to regulation of autophagy (Left). The exact pathways and genes are provided (Right). (C) The venn chart of miR-129-3p based on three classic target prediction database, miRWalk, miRDB and TargeScan. The top ten target genes in overlap part are shown in right panel. (D) The network generated from STRING database analysis and demonstrates the interaction between Atg4B and many other genes that play vital roles in autophagy mediation.

**Table 2**
GO enrichment and KEGG pathways of Atg4b.

| Gene symbol | GO Term/KEGG |
|---|---|
| Atg4b | BP_GO:0000045 ~ autophagic vacuole formation<br>BP_GO:0006914 ~ autophagy<br>BP_GO:0000422 ~ mitophagy<br>BP_GO:0016239 ~ positive regulation of marcroautopahgy<br>CC_GO:0016020 ~ membrane<br>CC_GO:0005737 ~ cytoplasm<br>KEGG_PATHWAY ~ mmu04140: Regulation of autophagy |

129-3p obviously increased the survival of intracellular BCG (Fig. 8); miR-129-3p antagomir inhibited proliferation of the bacteria. Collectively, miR-129-3p overexpression favors BCG survival by inhibiting autophagy in macrophages.

## 3. Material and methods

### 3.1. RNA sequencing

RAW264.7 cells were treated with 3-methyladenine (5 mM, 12 h) or rapamycin (50 nm, 2 h) and then total RNA was isolated by using TRIzol reagent (Sigma). Before small RNA libraries were constructed,

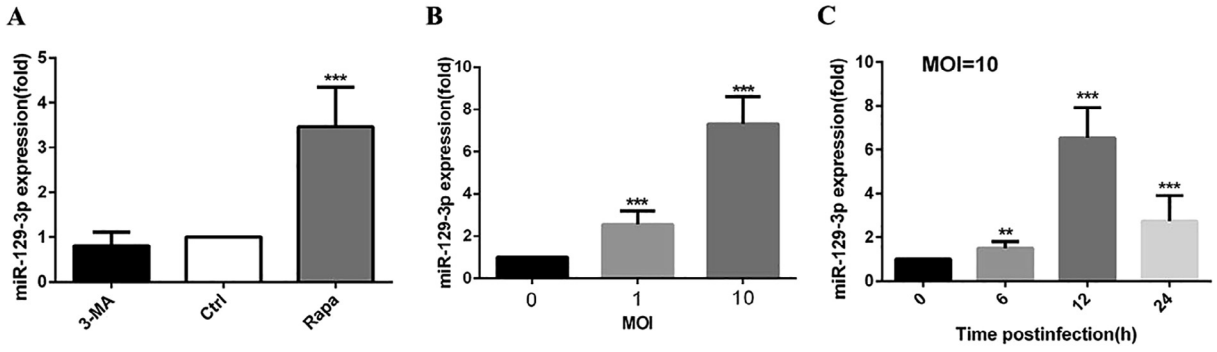


**Fig. 3.** BCG infection triggers miR-129-3p expression in RAW264.7 cell. (A) RAW264.7 cells were treated with 3-MA (5 mM, 12 h) or rapamycin (50 nm, 2 h), and the expression of miR-129-3p was measured by qRT-PCR. (B) RAW264.7 cells were infected with BCG at MOI of 1 or 10 for 6 h and miR-129-3p expression was detected by qRT-PCR. (C) Expression level of miR-129-3p in RAW264.7 cells that infected with BCG at MOI of 10 for 6H and the total RNA were isolated at indicate time. The expression of miR-129-3p was determined by qRT-PCR. Data represents the mean ± SD from three replications. $^{*}p < 0.05$, $^{**}p < 0.01$, $^{***}p < 0.001$.

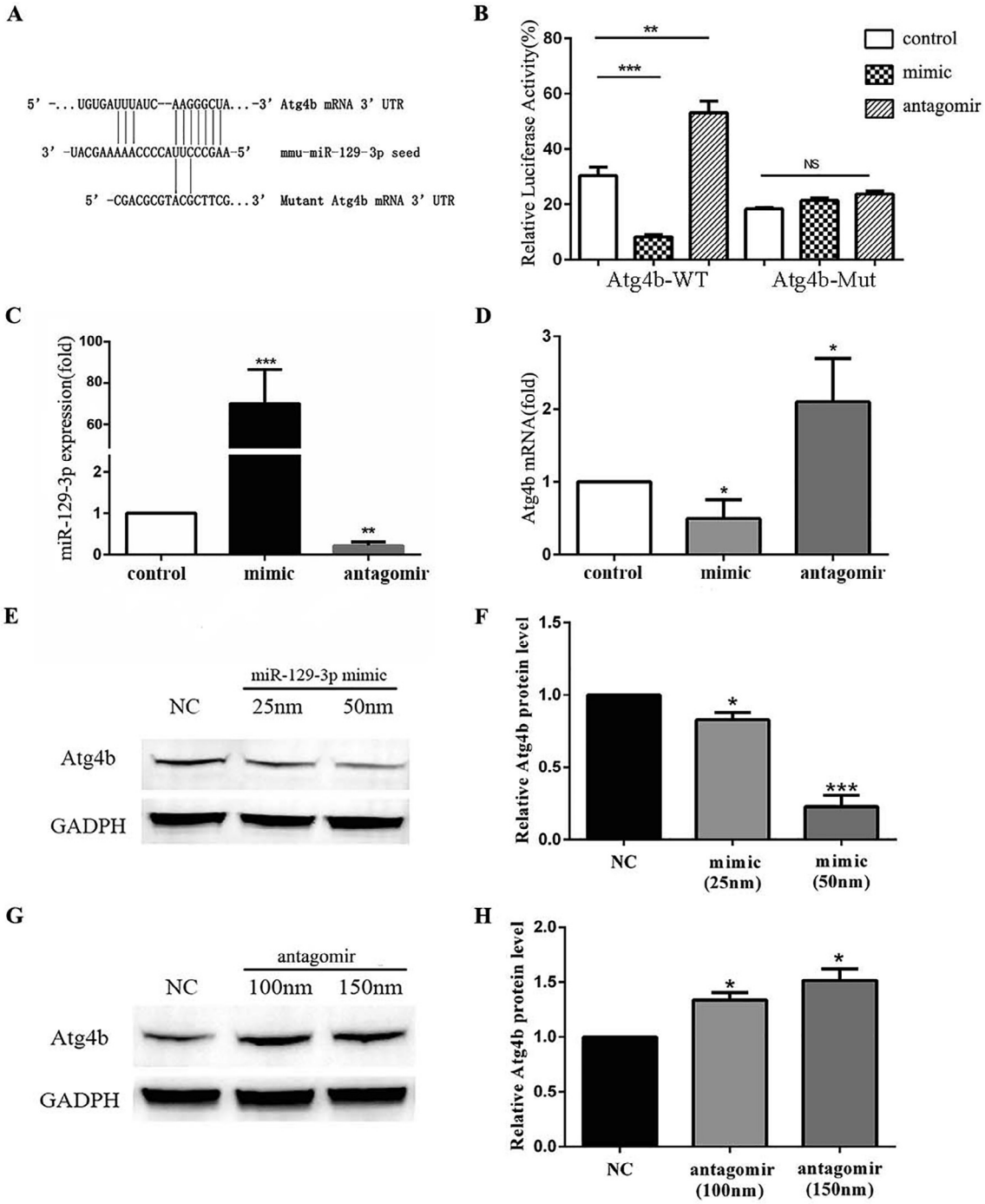


**Fig. 4.** MiR-129-3p reduce Atg4b expression by interacting of its 3′UTR. (A) The sequences of seed region obtained through target prediction analysis. The seed sequences of wild type and mutant of Atg4b was shown. (B) 293 T cells were transfected with control, mimic of miR-129-3p and wild type Atg4b or mutant Atg4b, antagomir of miR-129-3p and wild type Atg4b or mutant Atg4b reported plasmid. The luciferase activity was measured after 48H. Data represents the mean ± SD from three replications. $^{**}p < 0.01$, $^{***}p < 0.001$. (C) RAW264.7 cells were transfected with mimic or antagomir of miR-129-3p. The expression of miR-129-3p was detected by qRT-PCR. Data represents the mean ± SD from three replications. $^{**}p < 0.01$, $^{***}p < 0.001$. (D) RAW264.7 cells were transfected with mimic or antagomir of miR-129-3p for 24 h. The expression of Atg4b mRNA was determined by qRT-PCR. Data represent the mean ± SD from three replications. $^{*}p < 0.05$. (E) RAW264.7 cells were transfected with mimic of miR-129-3p at gradually increased concentration of 25 nm, 50 nm. The expression of Atg4b and GADPH were determined by Western Blot. (G) RAW264.7 cells were transfected with antagomir of miR-129-3p at gradually increased concentration of 100 nm or 150 nm. The expression of Atg4b and GADPH were determined by Western Blot. (F, H) Western blot results were analyzed by Image J software. Data represents the mean ± SD from three replications. $^{*}p < 0.05$, $^{***}p < 0.001$.

purity of total RNA was detected by Nanodrop to ensure OD260/OD280 ≥ 1.8; OD260/OD230 ≥ 1.0.Total RNA was measured by Qubit 2.0 to guarantee the concentration was above 250 ng/ul. Integrity of total RNA was tested by Agilent 2100 bioanalyzer (RIN ≥ 8.0, 25S/18S ≥ 1.5). The libraries was constructed strictly according to instruction of NEB Next Ultra small RNA Sample Library Prep Kit for Illumina (Illumina).Small RNAs were ligated with 5′RNA adaptor and 3′RNA adaptor. After first-strand synthesis and PCR amplification, target fragments were acquired by using gel separation technology. Before submitted to HiSeq2500, the concentration of the libraries was

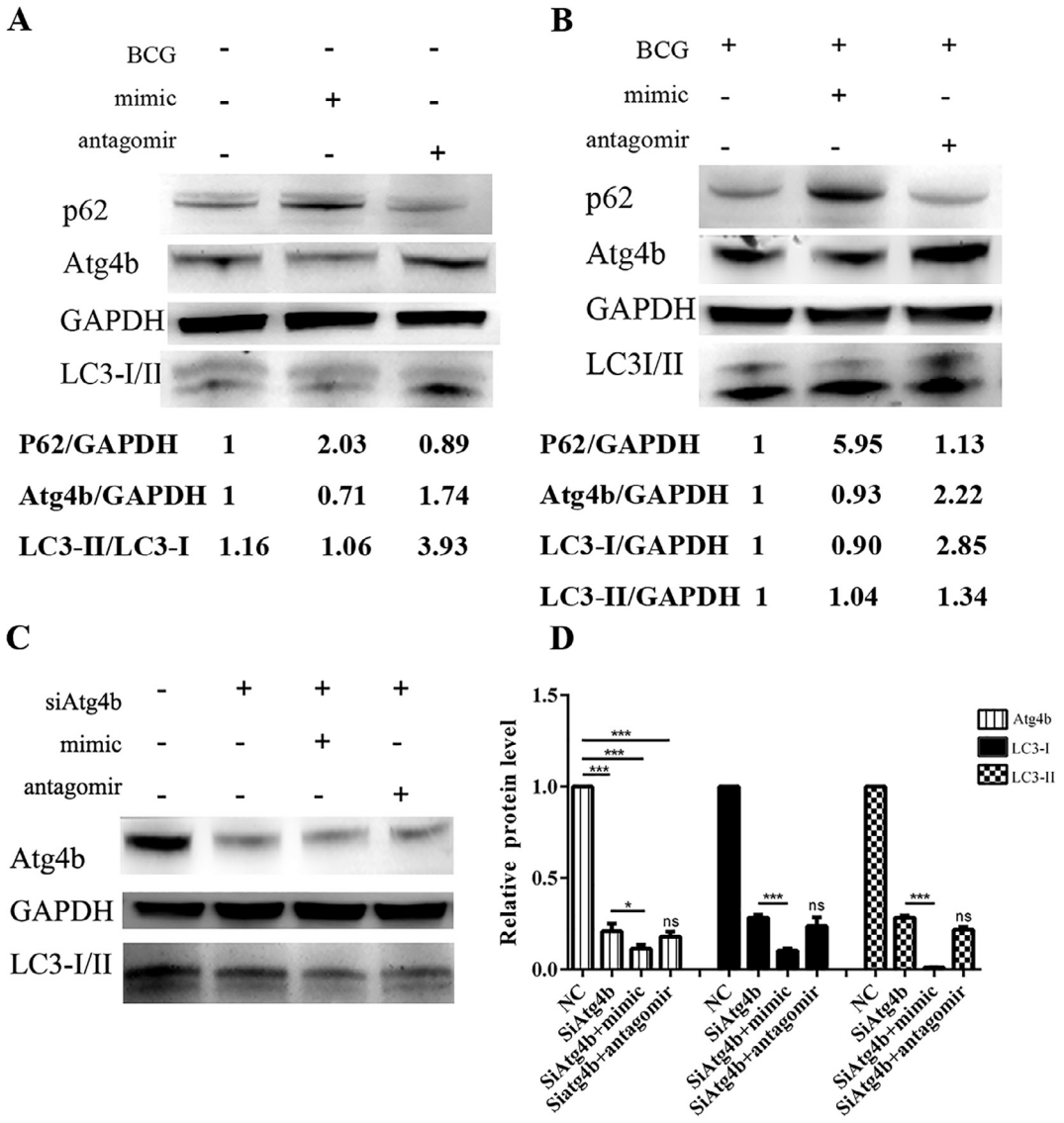


**Fig. 5.** MiR-129-3p suppresses autophagy in RAW264.7 cells by inhibiting Atg4b. (A) RAW264.7 cells were transfected with control, mimic or antagomir of miR-129-3p for 48 h, and the expression of P62, Atg4b, GADPH and LC3 were quantified by Western Blot. (B) RAW264.7 cells were transfected with control, mimic or antagomir of miR-129-3p for 24 h and then infected by BCG at MOI of 10 for 24 h. The expression of P62, Atg4b, GADPH and LC3 were measured by Western Blot. (C) RAW264.7 cells were transfected with control, siRNA of Atg4b, siRNA and mimic of miR-129-3p or antagomir of miR-129-3p. The quantity of *P*62, Atg4b, GADPH and LC3 was detected by Western Blot. (D) Western blot results were analyzed by Image J software. Data represents the mean ± SD from three replications. $^{*}p < 0.05$, $^{***}p < 0.001$.

detected by Qubit 2.0, Agilent 2100 bioanalyzer and Q-PCR. Sequencing was performed at Biomarker Technologies (Beijing). After comparing to Mouse reference genome (ftp://ftp.ensembl.org/pub/release-78/fasta/mus_musculus/) by using miRDeep2. The reads completely matching the mouse genome were collected for further enrichment .The differential expression of miRNAs were selected by |log2 (FC)| > = 1 FDR < = 0.01 as a standard.

### 3.2. Bioinformatics analysis of miRNAs

The differential expression of miRNAs was represented by heat map produced by Multi Experiment Viewer (MeV, http: //mev–multiple-experiment-viewer. sharewarejunction.com/). The potential target genes of miRNAs were predicted by miRDB (http://www.mirdb.org/miRDB/), miRanda (http://www.microRNA. org/) and Targetscan (http://www.targetscan.org/). The intersection of target genes from above three different databases was obtained by Venny 2.1(http://bioinfogp.cnb.csic.es/tools/venny/) which facilitated to acquire a venn diagram. Meanwhile, all predicted target genes (14570 genes) were upload to The Database for Annotation, Visualization and Integrated Discovery (DVIAD, https://david.ncifcrf.gov/), a efficient online program which could handle at most 3000 genes at a time with their functional annotations and pathway enrichment. Interaction between candidate proteins was predicted by using STRING, a functional protein association networks database (www.string-db.org/).

### 3.3. Cell culture and transfection

Murine macrophage RAW264.7 cells (ATCC; TIB-71) and HEK-293 T cells were purchased from the Type Culture Collection of the Chinese Academy of Sciences, Shanghai, China. The cells were maintained in DMEM medium contains 10% Fetal Bovine Serum (FBS) and incubated at 37 °C with 5% $CO_2$. RAW264.7 cells were transiently transfected with 50 nM control or miR-129-3p mimic (GenePharma, Shanghai, China);50 nM control or 150 nM miR-129-3p antagomir (GenePharma, Shanghai, China); or 50 pM Atg4b siRNA, using Lipofectamine 3000

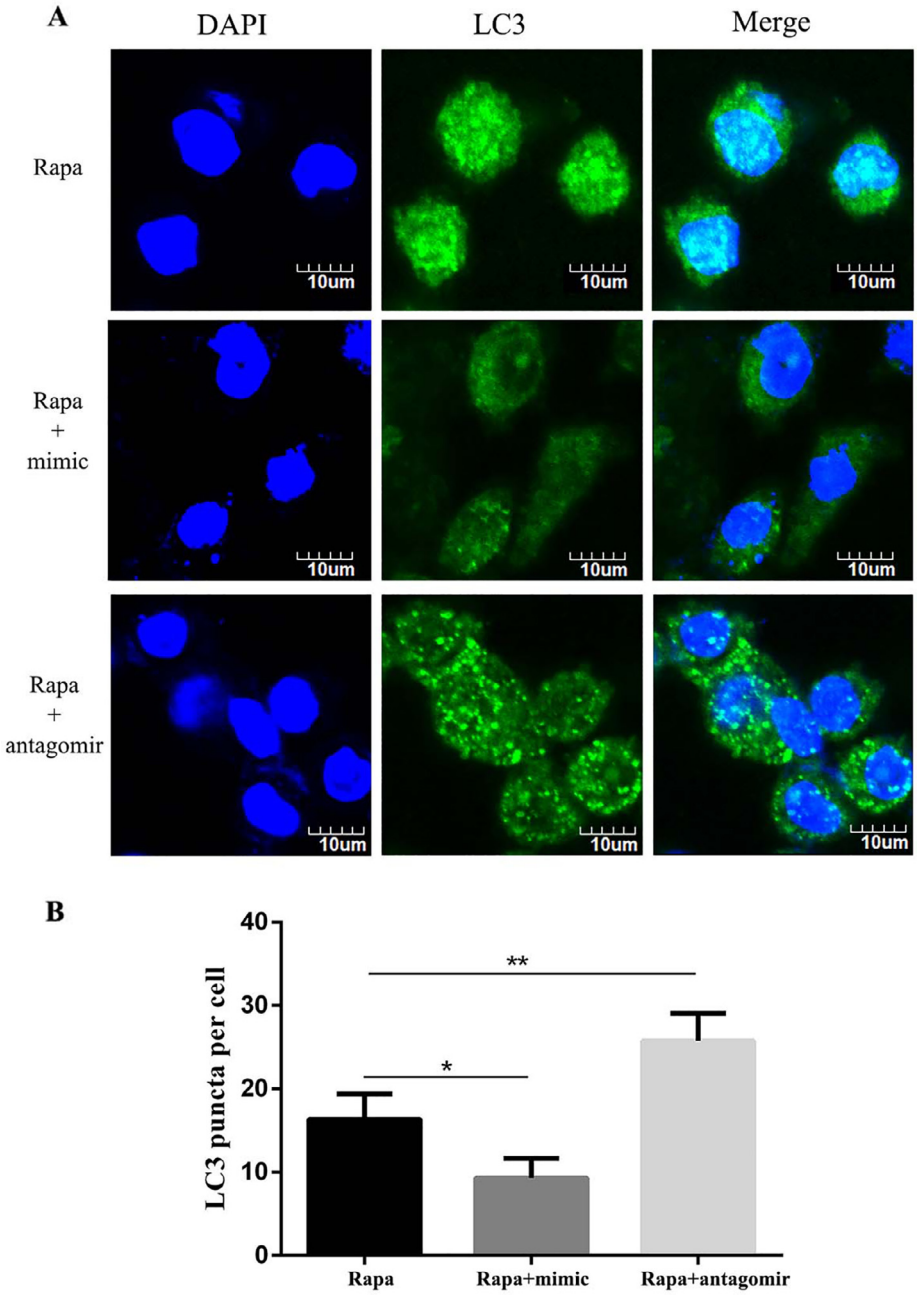


**Fig. 6.** MiR-129-3p impairs autophagy confirmed by immunofluorescence analysis. (A) The RAW264.7 cells were transfected with control, mimic or antagomir of miR-129-3p for 24 h and then treated with rapamycin for 2 h. Afterwards, the RAW264.7 cells were fixed and incubated in the presence of rabbit anti-LC3 antibody, followed by FITC-conjugated goat anti-rabbit IgG. LC3 puncta was determined by confocal microscopy at 60X objective lens. (B) LC3 puncta were counted. Data represents the mean ± SD from three replications. $^{*}p < 0.05$, $^{**}p < 0.01$.

(Invitrogen, USA) according to the manufacturer's instructions

### 3.4. Bacterial strains and CFU assays

Bacillus Calmette-Guérin (BCG) Beijing strain was purchased from Center for Disease Control and Prevention of China, and bacilli were grown in Middlebrook 7H9 with 10% albumin dextrose catalase (ADC) supplement at 37 °C for 20 days. The BCG were collected by centrifugation at 500 X g for 8 min, and resuspended with culture medium for cells infection. RAW264.7 cells was infected at MOI = 10 for six hours and then washed by PBS thrice. For CFU assays, RAW264.7 cells were transfected with agomir or antagomir of miR-129-3p for 24 h. Afterwards, cells were infected by the BCG bacilli suspension for 6 h. The extracellular BCG were removed by washing with PBS. The infected cells were incubate at 37 °C for another 24 h and lysed by cell lysis buffer. After that, quantitative culturing was performed with 10-fold serial dilutions on 7H10 agar plated with OADC. The plates were incubated at 37 °C for 3 weeks, and colonies were counted.

### 3.5. Plasmid construction and luciferase reporter assays

The wild-type 3′-UTR of Atg4b which covers the seed region of miR-129-3p was acquired by PCR. The mutant 3′-UTR of Atg4b was constructed via PCR based on the site-directed mutagenesis theory. The primers used in the study were provided in Table 3.These wild-type or mutant Atg4b 3′UTR were cloned into pMIR-Report vector (Ambion),

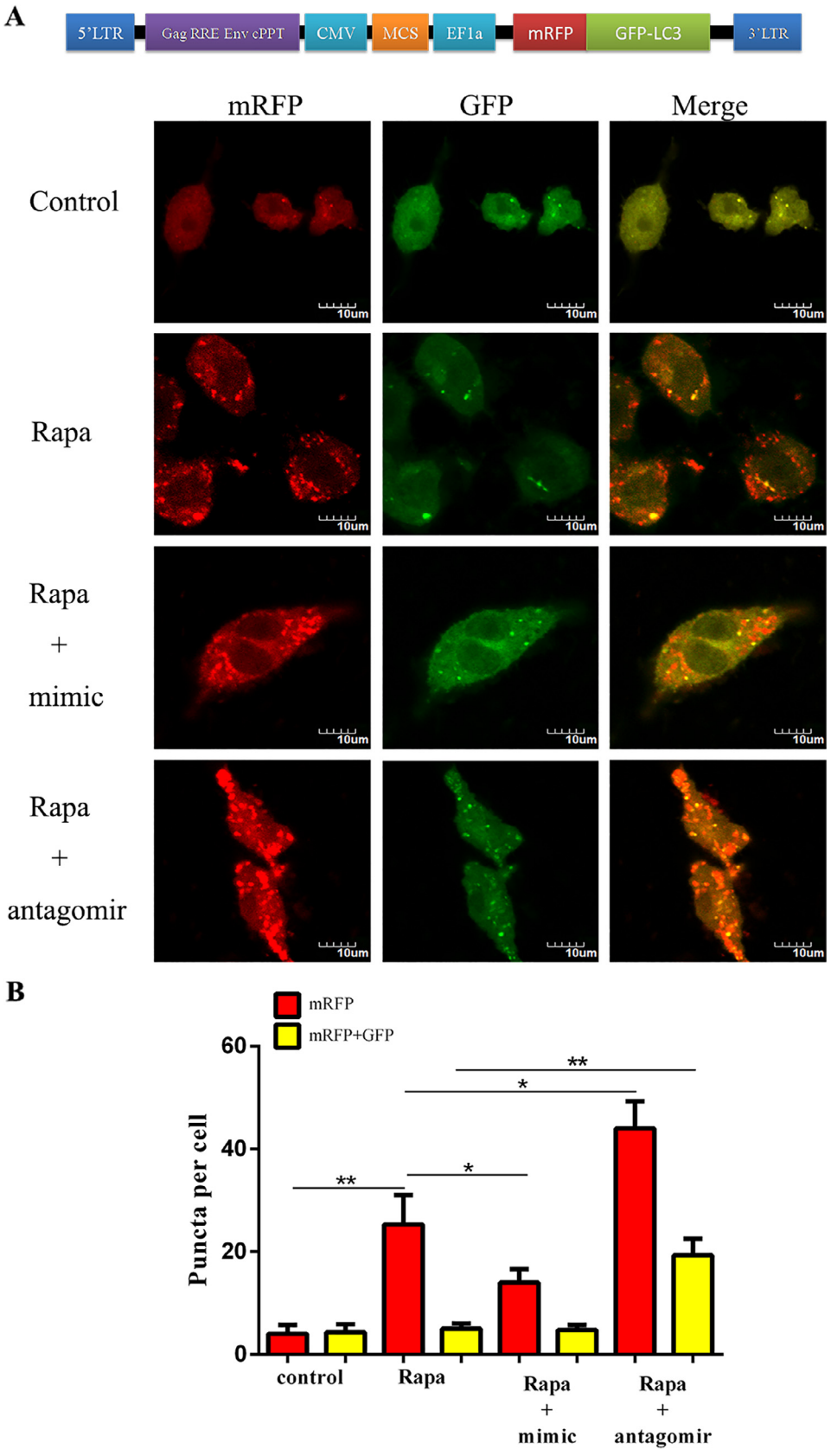


**Fig. 7.** MiR-129-3p restrains phagosome formation. (A) The RAW264.7 cells were transfected with control, mimic or antagomir of miR-129-3p for 24 h and then treated with rapamycin for 2 h. The pictures were captured by confocal microscope under 60 X objective lens. (B) The red or yellow puncta were counted by Image J software. Data represents the mean ± SD from three replications. $^{*}p < 0.05$, $^{**}p < 0.01$.

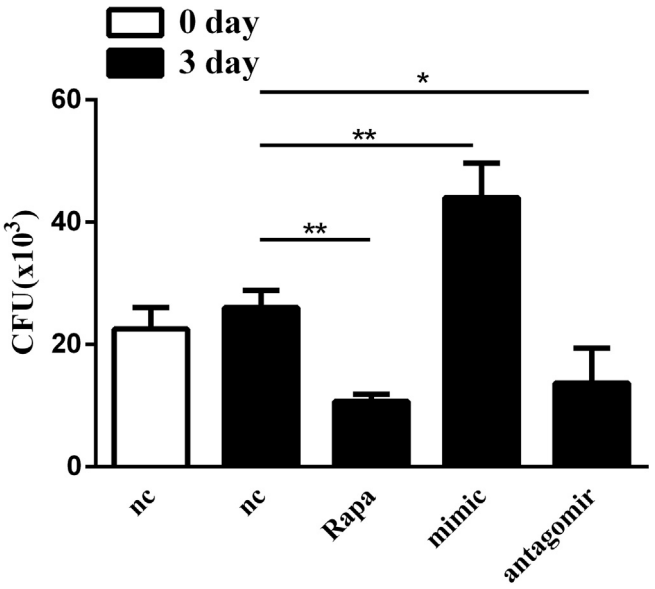


**Fig. 8.** MiR-129-3p overexpression favors BCG survival. RAW264.7 cells were transfected with control, mimic or antagomir of miR-129-3p. After that, cells were infected by BCG at MOI of 10.Intracellular survival of BCG were detected by CFU assay. Data are presented the mean ± SD from three replications. $^{*}p < 0.05$, $^{**}p < 0.01$.

**Table 3**
Primer information.

| Primers | Sequence (5′-3′) |
|---|---|
| miR-129-3p | RT Stem-loop: CTCAACTGGTGTCGTGGAGTCGGCAATTCAGTTGAG ATACTTTT<br>Forward: ACACTCCAGCTGGGAAGCCCTTACCCCAAA<br>Reverse: TGGTGTCGTGGAGTCG |
| Atg4b mRNA | Forward: CGAGCTCTGGGTCTGTGGTTTATTTG<br>Reverse: GACGCGTCTGGAGGAAGGCTCAAGTA |
| Atg4b-WT | Forward: CCGAGCTCTCCTGGGCACCTGGGTCTGT<br>Reverse: CGACGCGTCCAGTGGGCACGGTGTCTCA |
| Atg4b-Mut | Forward: CCGAGCTCTCCTGGGCACCTGGGTCTGT<br>Reverse: CGACGCGTACGCTTCGATAAATCACACTGGGCAGA |
| GAPDH | Forward: GCACCGTCAAGGCTGAGAAC<br>Reverse: TGGTGAAGACGCCAGTGGA |
| U6 | Forward: CTCGCTTCGGCAGCACA<br>Reverse: AACGCTTCACGAATTTGCGT |
| miR-129-3p mimic | AAGCCCUUACCCCAAAAAGCAU<br>GCUUUUUGGGGUAAGGGCUUUU |
| miR-129-3p antagomir | AUGCUUUUUGGGGUAAGGGCUU |
| NC | Forward: UUCUCCGAACGUGUCACGUTT<br>Reverse: ACGUGACACGUUCGGAGAATT |

producing pMIR-Report-Atg4b-WT (Atg4b-WT) or pMIR- Report-Atg4b-Mut (Atg4b-Mut). Plasmids Atg4b-WT or Atg4b-Mut was cotransfected with control, agomir or antagomir of miR-129-3p into 293 T cells with Lipofectamine 2000 (Invitrogen). In addition, each group was transfected with pRL-TK (purchased from Promege) at the same time as a reference for evaluating transfection efficiency. The relative activity of firefly luciferase at 48 h post-transfection was determined by the Dual-Luciferase Reporter Assay System (Promega) following the manufacturer's protocol.

### 3.6. Quantitative Real-Time PCR

The expression of miR-129-3p in RAW264.7 cells were detected through qRT-PCR. Total RNA was obtained by using TRIzol reagent (Sigma). For measuring, cDNA was synthesized by using RevertAid Fisrt Strand cDNA Synthesis kit (ThermoFisher Scientific) and qRT-PCR was performed by using SYBR Select Master Mix (Applied Biosystems). RNU6 (for miRNA detecting) or GAPDH (used in mRNA detecting) gene was used for normalization. The primers used in qRT-PCR are shown in Table 3.The PCR cycle were as follows: 95∘C for30s, 40 cycles of 95 ∘C for15s, followed by 60 ∘C for 30 s and 72∘C for 30 s. The quantity was calculated by using a comparative Ct (△△Ct) method.

### 3.7. Western-Blot

Proteins were loaded onto 12% SDS-PAGE gels and transferred to a polyvinylidene difluoridemembrane (PVDF, Millipore, USA). Membranes were incubated in 5% BSA which contains antibody of Atg4b, LC3B, SQSTMT/*P*62, or GAPDH (purchased from Cell Signaling Technology)for 12–16 h.After that, the membranes were washed by TBST three times and then incubated with HRP-conjugated goat anti-rabbit IgG secondary antibody for 1 h. Ultimately, immunoreactive band analysis was performed by using ECL reagent (Thermo Fisher Scientific).

### 3.8. Confocal microscopy

The RAW264.7 cells were transfected with miR-129-3p mimic, antagomir and control for 48 h. After that, cells were fixed with 4% para formaldehyde and 0.2% Triton X-100. After blocked by 5% bovine serum albumin, cells were incubated with Rabbit anti-LC3 antibody and then FITC-conjugated goat anti-rabbit IgG. The images of cells were acquired by using Olympus DSU spinning disk confocal microscope under 60 X objective lens.

### 3.9. Cell strain expressing mRFP-GFP-LC3 plasmid

The RAW264.7 cells were transduced with lentiviral system encoding mRFP-GFP-LC3 plasmid which constructed by us previously. The positive cells were isolated by using FCM and preserved properly as a strain. The cells were then transfected with miR-129-3p mimic or antagomir, and the photograph of cells were captured by confocal microscope under 60 X objective lens.

### 3.10. Statistical analysis

All of the results are presented as mean ± SD of independent experiments. Statistical analyses were performed by using two-tailed Student's *t*-test. ANOVA was recruited to analyze comparisons between groups. Significant differences were assigned to p values $< 0.05$, $< 0.01$ and $< 0.001$, denoted by $^{*}$, $^{**}$ and $^{***}$, respectively.

## 4. Discussion

MTB is the causative pathogen of tuberculosis which is one of the toughest infectious diseases. The conflicts between host immune system and pathogenic infection are more like a war. Each side has regular tactics of struggle against the enemy. Obviously, macrophages are the first defensive line against MTB through initiating host inflammatory response. Among these responses, autophagy undoubtedly plays vital roles. However, MTB can fight back by evading host immune scanner and attacks of macrophages. For instance, MTB prevents the fusion of autophagosome and lysosome, which deceases the sensitivity of macrophages responding to infection stimulation [27]. Furthermore, the self-protecting strategy of MTB seems been developed as studies go deeper. A new research revealed the MTB can inhibit fusion process as well as reprogram host lipid metabolism, suggesting that MTB might survive in autophagosome with lipid riche niche as a source of energy [5]. In addition, an increasing number of miRNAs are proved to correlate with autophagy as regulators in MTB infection. For instance, miR-155 could manipulate by MTB to regulate Atg3 for its own survival

[28]. Nonetheless, the molecular mechanism of autophagy in mediating MTB clearance is still worthy to explore. In this study, a novel miR-129-3p was found through bioinformatics methods and could inhibit autophagy through interacting with Atg4b and promote BCG survival in macrophages, which may offer a better understanding of MTB persistent infection.

Speaking of finding new miRNAs we are interested in, bioinformatics analysis cannot be ignorant. At the beginning of our research, High-throughput sequencing was employed to identify differential expression of miRNAs in treatment of 3-MA or rapamycin groups. After RNA-sequencing, as shown in Fig. 1A, differential expression of miRNAs suggest that they may play important roles in autophagy regulation. Notably, some of these miRNAs have been proved as the regulator of autophagy. For example, hypoxia-induced autophagy is mediated by miR-210 through HIF-1/BCL-2 pathway in human colon cancer cells [29]. MiR-20a-5p could inhibit cell proliferation and induce apoptosis by down-regulate Atg5 and thereby inhibit autophagy in SH-SY5Y cells [30]. Furthermore, over expression of miR-129-5p results in the suppression of Beclin-1 thus impair the protective effects of endothelial cell autophagy [31]. MiR-181a reduces rapamycin- and starvation-induced autophagy by interacting with the 3′UTR of Atg5 [3]. MiR-155 could increase autophagic activity by targeting Rheb and favor elimination of intracellular MTB [4]. Taken together, our methods to find novel miRNAs that will be involved in autophagy supposed to be reliable. After serial bioinformatics analysis and verifying, we found miR-129-3p is down-expressed in 3-MA group while is up expressed in rapamycin treatment group, which means it maybe have influence on autophagy.

Autophagy-related genes (ATG) are a number of genes that involved in regulation of autophagy. Among these genes, Atg4b unquestionably play vital role in this process. Reports indicate that Atg4b could mediate lipidation or delipidation of LC3-II, as well as the crosstalk between LC3-modification and Atg12-conjugation [32]. More researchers showed that the Atg4b-deficient mice displayed higher inflammatory response, which means ATG4B protease and autophagy are crucial protecting epithelial cells against apoptosis and in the regulation of inflammatory and fibrotic response [33] and other researchers reported that the down-regulation of ATG4B regulated by miR-34a/34c-5p could suppress autophagy which was induced by rapamycin [34]. Our results showed decreased expression of Atg4b in RAW264.7 cells by transfecting with siRNA of Atg4b significantly decreased expression of both LC3-I and LC3-II, resulting in LC3-II/I ratio change. This may because proLC3 was cleavaged to expose GLY by hAtg4B, and then transformed into LC3-I [32]. What‘s more, in our study, we found miR-129-3p had potential ability to interact with 3′UTR of Atg4b using TargetScan. Mimic of miR-129-3p negatively regulates luciferase activity in 293 T cells containing Atg4b-WT vector while luciferase activity in 293 T cells transfected with Atg4b-Mut vector has no change. Consistently, qRT-PCR and western blotting assays showed that miR-129-3p significantly suppressed Atg4b expression both in protein and mRNA level. Besides, miR-129-3p mimic or antagomir can‘t enhance or rescue Atg4b expression in RAW264.7 cells transfected with siRNA of Atg4b. And those demonstrate that miR-129-3p could directly target Atg4b, and then impress the following processes including autophagy, wich is one of the innate defenses against MTB infection [35]. Follow on upon study of the association between miR-129-5p, Our study indicated that miR-129-3p could suppress autophagy. It could decrease LC3-II/I ratio in accordance with elevating p62 expression in both non- or BCG-infected RAW264.7 cells, and significantly reduce LC3 puncta in RAW264.7 cells. Since macrophages are habitats of MTB resident and autophagy appeared as host defenses of infectious agents like MTB [36,37].We further studied the impact of miR-129-3p on the BCG survival in RAW264.7 cells,and the results showed transfected miR-129-3p overexpression could promote the BCG survival in RAW264.7 while its down expression restricted it.

Numerous studies dedicated on the research about the relationship around miRNAs, autophagy and MTB infection. In this study, we found a novel miRNA, miR-129-3p, is benefit for the BCG‘s intracellular survival in RAW264.7 cells through targeting Atg4b and suppressing autophagy. This study added proofs that miRNAs is important in the development of autophagy and TB infection, and made miR-129-3p ,which is interacting with Atg4b, becoming a potential target for the treatment of TB diseases.

## 5. Conclusion

Altogether, our data suggested that miR-129-3p was involved in regulation of autophagy as an inhibitor and favored intracellular BCG survival by suppressing Atg4b in RAW264.7 cells. This study provides a systematic bioinformatics analysis process for locking the objective we interested in along with a better understanding of MTB resistant and persistent infection.

## Funding

The study was funded by the National Natural Science Foundation of China (No. 31472168), 2015 Ningxia Scientific and technological innovation leader training project (KJT2015020), First-class Discipline construction of clinical medicine of Ningxia Medical University (NXYLXUK2017A05) and Natural Science Foundation of Ningxia (2018AAC03084).

## References

[1] R.K. Pai, M. Convery, T.A. Hamilton, W.H. Boom, C.V. Harding, Inhibition of IFN-γ-Induced Class II Transactivator Expression by a 19-kDa Lipoprotein from Mycobacterium tuberculosis: A Potential Mechanism for Immune Evasion, J. Immunol. 171 (1) (2003) 175–184.
[2] J. Rengarajan, E. Murphy, A. Park, C.L. Krone, E.C. Hett, B.R. Bloom, L.H. Glimcher, E.J. Rubin, Mycobacterium tuberculosis Rv2224c modulates innate immune responses, PNAS 105 (1) (2008) 264–269.
[3] K.A. Tekirdag, G. Korkmaz, D.G. Ozturk, R. Agami, D. Gozuacik, MIR181A regulates starvation- and rapamycin-induced autophagy through targeting of ATG5, Autophagy 9 (3) (2013) 374–385.
[4] J. Wang, K. Yang, L. Zhou, Wu.Y. Minhaowu, M. Zhu, X. Lai, T. Chen, L. Feng, M. Li, et al., MicroRNA-155 promotes autophagy to eliminate intracellular mycobacteria by targeting Rheb, PLoS Pathog. 9 (10) (2013) e1003697.
[5] M. Ouimet, S. Koster, E. Sakowski, B. Ramkhelawon, C. van Solingen, S. Oldebeken, D. Karunakaran, C. Portal-Celhay, F.J. Sheedy, T.D. Ray, et al., Mycobacterium tuberculosis induces the miR-33 locus to reprogram autophagy and host lipid metabolism, Nat. Immunol. 17 (6) (2016) 677–686.
[6] D.P. Bartel, MicroRNAs: genomics, biogenesis, mechanism, and function, Cell 116 (2004) 281–297.
[7] G. Walzl, M.C. Haks, S.A. Joosten, L. Kleynhans, K. Ronacher, T.H. Ottenhoff, Clinical immunology and multiplex biomarkers of human tuberculosis, Cold Spring Harbor Perspect. Med. 5 (4) (2014).
[8] J. Wei, X. Huang, Z. Zhang, W. Jia, Z. Zhao, Y. Zhang, X. Liu, G. Xu, MyD88 as a target of microRNA-203 in regulation of lipopolysaccharide or Bacille Calmette-Guerin induced inflammatory response of macrophage RAW264.7 cells, Mol. Immunol. 55 (3–4) (2013) 303–309.
[9] G. Romano, L.N. Kwong, Diagnostic and therapeutic applications of miRNA-based strategies to cancer immunotherapy, Cancer Metastasis Rev. (2017).
[10] I.A. Ciechomska, C.G. Goemans, A.M. Tolkovsky, Molecular links between autophagy and apoptosis, in: V. Deretic, N.J. Totowa (Eds.), Autophagosome and Phagosome, Humana Press, 2008, pp. 175–193.
[11] G. Wan, W. Xie, Z. Liu, W. Xu, Y. Lao, N. Huang, K. Cui, M. Liao, J. He, Y. Jiang, et al., Hypoxia-induced MIR155 is a potent autophagy inducer by targeting multiple players in the MTOR pathway, Autophagy 10 (1) (2014) 70–79.
[12] J.K. Kim, H.M. Lee, K.S. Park, D.M. Shin, T.S. Kim, Y.S. Kim, H.W. Suh, S.Y. Kim, I.S. Kim, J.M. Kim, et al., MIR144* inhibits antimicrobial responses against Mycobacterium tuberculosis in human monocytes and macrophages by targeting the autophagy protein DRAM2, Autophagy 13 (2) (2017) 423–441.
[13] L. Li, Y.Y. Chen, S.Q. Li, C. Huang, Y.Z. Qin, Expression of miR-148/152 family as potential biomarkers in non-small-cell lung cancer, Med. Sci. Monit. : Int. Med. J. Exp. Clin. Res. 21 (2015) 1155–1161.
[14] F. Wang, H. Ying, B. He, Y. Pan, H. Sun, S. Wang, Circulating miR-148/152 family as potential biomarkers in hepatocellular carcinoma, Tumor Biol. 37 (4) (2016) 4945–4953.
[15] D.W. Huang, B.T. Sherman, Q. Tan, J. Kir, D. Liu, D. Bryant, Y. Guo, R. Stephens, M.W. Baseler, H.C. Lane, et al., DAVID Bioinformatics Resources: expanded annotation database and novel algorithms to better extract biology from large gene lists, Nucl. Acids Res. 35 (Web Server issue) (2007) W169-175.
[16] L. Guo, J. Zhao, Y. Qu, R. Yin, Q. Gao, S. Ding, Y. Zhang, J. Wei, G. Xu, microRNA-20a Inhibits Autophagic Process by Targeting ATG7 and ATG16L1 and Favors

Mycobacterial Survival in Macrophage Cells, Front. Cell. Infect. Microbiol. 6 (2016) 134.
[17] M. Liang, Z. Habib, K. Sakamoto, X. Chen, G. Cao, Mycobacteria and autophagy: many questions and few answers, Curr. Issues Mol. Biol. (2017).
[18] E. Tasdemir, M.C. Maiuri, L. Galluzzi, I. Vitale, M. Djavaheri-Mergny, M. D'Amelio, A. Criollo, E. Morselli, C. Zhu, F. Harper, et al., Regulation of autophagy by cytoplasmic p53, Nat. Cell Biol. 10 (6) (2008) 676–687.
[19] L. You, Z. Wang, H. Li, J. Shou, Z. Jing, J. Xie, X. Sui, H. Pan, W. Han, The role of STAT3 in autophagy, Autophagy 11 (5) (2015) 729–739.
[20] K.J. Petherick, O.J.L. Conway, C. Mpamhanga, S.A. Osborne, A. Kamal, B. Saxty, I.G. Ganley, Pharmacological inhibition of ULK1 kinase blocks mammalian target of rapamycin (mTOR)-dependent autophagy, J. Biol. Chem. 290 (48) (2015) 28726–28726.
[21] C. He, M.C. Bassik, V. Moresi, K. Sun, Y. Wei, Z. Zou, Z. An, J. Loh, J. Fisher, Q. Sun, et al., Exercise–induced BCL2–regulated autophagy is required for muscle glucose homeostasis, Nature 481 (7382) (2012) 511–515.
[22] J.K. Kim, J.M. Yuk, S.Y. Kim, T.S. Kim, H.S. Jin, C.S. Yang, E.K. Jo, MicroRNA-125a inhibits autophagy activation and antimicrobial responses during mycobacterial infection, J. Immunol. 194 (11) (2015) 5355–5365.
[23] A.I. Rovetta, D. Peña, R.E. Hernández Del Pino, G.M. Recalde, J. Pellegrini, F. Bigi, R.M. Musella, D.J. Palmero, M. Gutierrez, M.I. Colombo, et al., IFNG-mediated immune responses enhance autophagy against Mycobacterium tuberculosis antigens in patients with active tuberculosis, Autophagy 10 (12) (2014) 2109–2121.
[24] N. Fujita, M. Hayashi-Nishino, H. Fukumoto, H. Omori, A. Yamamoto, T. Noda, T. Yoshimori, An Atg4B mutant hampers the lipidation of LC3 paralogues and causes defects in autophagosome closure, Mol. Biol. Cell 19 (11) (2008) 4651–4659.
[25] K. Cadwell, J. Liu, S.L. Brown, H. Miyoshi, J. Loh, J. Lennerz, C. Kishi, W. Kc, J.A. Carrero, S. Hunt, et al., A unique role for autophagy and Atg16L1 in Paneth cells in murine and human intestine, Nature 456 (7219) (2008) 259–263.
[26] G. Korkmaz, K.A. Tekirdag, D.G. Ozturk, A. Kosar, O.U. Sezerman, D. Gozuacik, MIR376A is a regulator of starvation-induced autophagy, PLoS One 8 (12) (2013) e82556.
[27] A. Romagnoli, M.P. Etna, E. Giacomini, M. Pardini, M.E. Remoli, M. Corazzari, L. Falasca, D. Goletti, V. Gafa, R. Simeone, et al., ESX-1 dependent impairment of autophagic flux by Mycobacterium tuberculosis in human dendritic cells, Autophagy 8 (9) (2012) 1357–1370.
[28] M.P. Etna, A. Sinigaglia, A. Grassi, E. Giacomini, A. Romagnoli, M. Pardini, M. Severa, M. Cruciani, F. Rizzo, E. Anastasiadou, et al., Mycobacterium tuberculosis-induced miR-155 subverts autophagy by targeting ATG3 in human dendritic cells, PLoS Pathog. 14 (1) (2018) e1006790.
[29] Y. Sun, X. Xing, Q. Liu, Z. Wang, Y. Xin, P. Zhang, C. Hu, Y. Liu, Hypoxia-induced autophagy reduces radiosensitivity by the HIF-1alpha/miR-210/Bcl-2 pathway in colon cancer cells, Int. J. Oncol. 46 (2) (2015) 750–756.
[30] Y. Yu, J. Zhang, Y. Jin, Y. Yang, J. Shi, F. Chen, S. Han, P. Chu, J. Lu, H. Wang, et al., MiR-20a-5p suppresses tumor proliferation by targeting autophagy-related gene 7 in neuroblastoma, Cancer Cell Int. 18 (2018) 5.
[31] Z. Geng, F. Xu, Y. Zhang, MiR-129-5p-mediated Beclin-1 suppression inhibits endothelial cell autophagy in atherosclerosis, Am. J. Transl. Res. 8 (4) (2016) 1886–1894.
[32] I. Tanida, T. Ueno, E. Kominami, LC3 conjugation system in mammalian autophagy, Int. J. Biochem. Cell Biol. 36 (12) (2004) 2503–2518.
[33] S. Cabrera, M. Maciel, I. Herrera, T. Nava, F. Vergara, M. Gaxiola, C. López-Otín, M. Selman, A. Pardo, Essential role for the ATG4B protease and autophagy in bleomycin-induced pulmonary fibrosis, Autophagy 11 (4) (2015) 670–684.
[34] Y. Wu, X. Dai, Z. Ni, X. Yan, F. He, J. Lian, The downregulation of ATG4B mediated by microRNA-34a/34c-5p suppresses rapamycin-induced autophagy, Iranian J. Basic Med. Sci. 20 (10) (2017) 1125–1130.
[35] R.S. Rekha, S.S.V.J. Rao Muvva, M. Wan, R. Raqib, P. Bergman, S. Brighenti, G.H. Gudmundsson, B. Agerberth, Phenylbutyrate induces LL-37-dependent autophagy and intracellular killing of Mycobacterium tuberculosis in human macrophages, Autophagy 11 (9) (2015) 1688–1699.
[36] G. Xu, J. Wang, G.F. Gao, C.H. Liu, Insights into battles between Mycobacterium tuberculosis and macrophages, Protein Cell 5 (10) (2014) 728–736.
[37] L. Espert, B. Beaumelle, I. Vergne, Autophagy in Mycobacterium tuberculosis and HIV infections, Front. Cell. Infect. Microbiol. 5 (2015) 49.
[38] David J. Gregory, Igor Kramnik, Lester Kobzik, Protection of macrophages from intracellular pathogens by miR-182-5p Mimic—a gene expression meta-analysis approach, FEBS J. 285 (2) (2018) 244–260.
[39] Luo Jing, Jie Chen, Li He, Mir-129-5p, attenuates irradiation-induced autophagy and decreases radioresistance of breast cancer cells by targeting HMGB1, Int. Med. J. Exp. Clin. Res. 21 (2015) 4122–4129.